Vol 16 No 6, June 2007
1009-1963/2007/16(06)/1650-05

Chinese Physics

© 2007 Chin. Phys. Soc.
and IOP Publishing Ltd

UV and visible upconversion luminescence in Er^{3+}:YAG under red laser excitation*

Yang Hai-Gui(杨海贵), Dai Zhen-Wen(戴振文), and Zu Ning-Ning(祖宁宁)

Department of Physics, Jilin University, Key Laboratory of Coherent Light, Atomic and Molecular Spectroscopy, Ministry of Education, Changchun 130023, *China*

(Received 27 October 2006; revised manuscript received 13 November 2006)

This paper reports that the ultraviolet and visible upconversion luminescence from the $^4S_{3/2}$, $^2G_{9/2}$ and $^2P_{3/2}$ levels have been observed in Er^{3+}:YAG following 647.2 nm excitation of the $^4F_{9/2}$ multiple. Upconversion luminescence intensity dependence on pump power was recorded. The measured decay profiles were theoretically fitted by kinetics theory and the basically good agreements were achieved. The results indicate that some energy transfer processes proposed to explain the observed upconversion phenomena are reasonable.

Keywords: upconversion, luminescence dynamics, Er^{3+}:YAG
PACC: 3220J, 4265K, 7630K

1. Introduction

In the last decade, due to wide applications of short-wavelength solid-state lasers from ultraviolet (UV) to green spectral range, much attentions have been devoted to upconversion studies in rare earth (RE) ion-doped materials.[1−5] The upconversion phenomenon can provide a potential of producing attractive UV and vacuum UV upconversion lasers by using the intrinsic energy level matching of certain RE ions,[5,6] which does not need either stringent phase matching or high excitation wavelength stability as harmonic generation does. Moreover visible photon pumping will reduce photoionization and colour-centre formation effects observed under intense UV one-photon pumping. Upconversion provides an opportunity for exploring compact, all solid-state lasers in the UV and violet ranges with the rapid development of low-cost high-energy diode lasers.

Upconversion studies have focused on trivalent RE ions in various solid hosts. Among all the RE ions, Er^{3+} is one of the most popular and most efficient ions due to the abundant energy levels in the IR (infrared) - UV range. Especially, the important absorption bands in the emission domain of the laser diodes indicate that the Er^{3+} doped crystals are very convenient systems for upconversion laser. The visible upconversion luminescence of Er^{3+} ion has been investigated extensively in many kinds of host materials and visible upconversion laser has also been achieved in several Er^{3+}-doped materials under IR laser excitation.[7−12] Under red laser excitation of $^4F_{9/2}$, visible upconversion luminescence has also been detected in Er^{3+}-doped LaF_3, $LiTaO_3$ and $Ca_3Al_2Ge_3O_{12}$ crystals and sol-gel silica glass.[13−16] The dynamics of UV and visible upconversion in Er^{3+}:YAG was investigated under one- and two-colour excitations of $^4F_{9/2}$.[17]

In this paper, we study UV and visible upconversion luminescence in Er^{3+}:YAG under 647.2 nm excitation of $^4F_{9/2}$. Upconversion emission spectra and excitation spectra were presented as well as upconversion intensity dependence. Energy transfer processes were proposed to explain the observed upconversion phenomena. Some luminescence decay profiles were recorded by the time-resolved spectroscopy method and were theoretically fitted with the rate equation theory.

2. Experiment

The dopant concentration of Er^{3+}:YAG crystal used in our experiment is 10.5 at.%, which was grown by a conventional Czochralski method. Its size is 10×10×8 mm^3. YAG has a cubic space-group symmetry O_h^{10} and all 24 Y^{3+} ions occupy dodecahedral c sites with D_2 symmetry. The Er^{3+} dopant ions substi-

*Project supported by the National Natural Science Foundation of China (Grant No 10074020).
†Corresponding author. E-mail: dai@jlu.edu.cn

tute for Y^{3+} ions. Fig.1 gives the energy level diagram of Er^{3+} ions in YAG crystal based on the spectroscopic data reported by Gruber *et al.*[18]

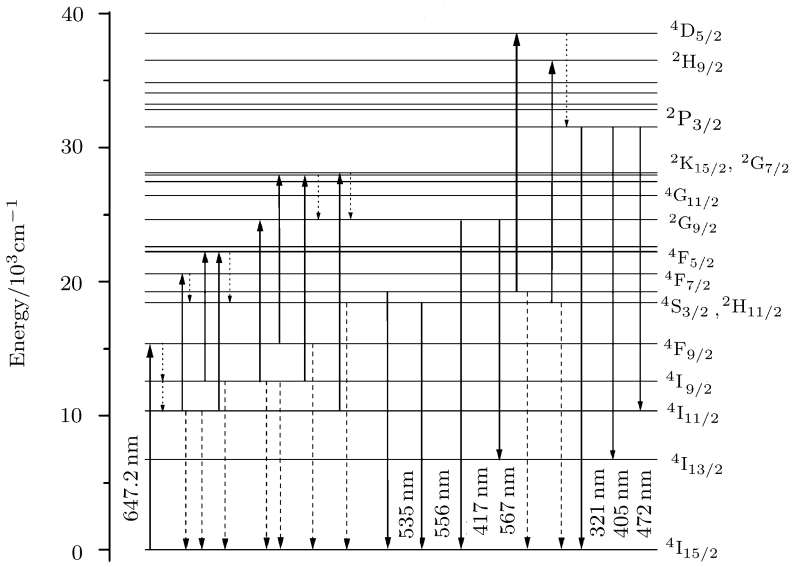


Fig.1. Energy level diagram Er^{3+} ions in YAG showing upconversion mechanisms and emission transitions.

In our experiment the sample was excited by a dye laser (Sirah Cobra-Stretch) with DCM dye which was pumped by a third harmonic of Nd:YAG laser (Spectra-Physics Quanta-Ray Pro-Series) with a 10 Hz repetition and a 10 ns pulse duration. The output from the dye laser is tunable from 614 nm to 673 nm. The pulse energy is about 3 mJ and the diameter is about 1.5 mm. The laser wavelength was calibrated by a pulsed wavelength meter (Burleigh WA-4500). The upconversion fluorescence was collected by a lens ($f = 15$ cm) in a direction perpendicular to the exciting beam, filtered by a 0.5 m monochromator with a resolution of 0.1 nm and detected by a photomultiplier tube (Hamamatsu R3896). The time-resolved fluorescence decay signals from the detector were recorded by a digital oscilloscope (Tektronix TDS 620B 500MHz) and processed by a boxcar integrator (Stanford Research Systems SR250). All experiments were performed at room temperature.

3. Results and discussion

Figure 2 shows the upconversion luminescence spectra of Er^{3+}:YAG under 647.2 nm excitation of $^4F_{9/2}$. UV and visible upconversion luminescence bands were observed. By means of the measured fluorescence decay profiles and the energy level data given by Gruber *et al*,[18] we give the assignment of upconversion luminescence bands around 321 nm ($^2P_{3/2} \rightarrow {}^4I_{15/2}$), 405 nm ($^2P_{3/2} \rightarrow {}^4I_{13/2}$), 417 nm ($^2G_{9/2} \rightarrow {}^4I_{15/2}$), 472 nm ($^2P_{3/2} \rightarrow {}^4I_{11/2}$), 535 nm ($^2H_{11/2} \rightarrow {}^4I_{15/2}$), 556 nm ($^4S_{3/2} \rightarrow {}^4I_{15/2}$) and 567 nm ($^2G_{9/2} \rightarrow {}^4I_{13/2}$). Fig.3 shows the excitation spectra from 643.5 to 658.5 nm at 417 and 556 nm upconversion luminescence, which have been calibrated by the laser power. Three optimal peaks of these spectra locate at the positions of 647.2, 652.2 and 655.2 nm. Here, the 647.2 nm exciting laser was chosen for the upconversion studies in this work.

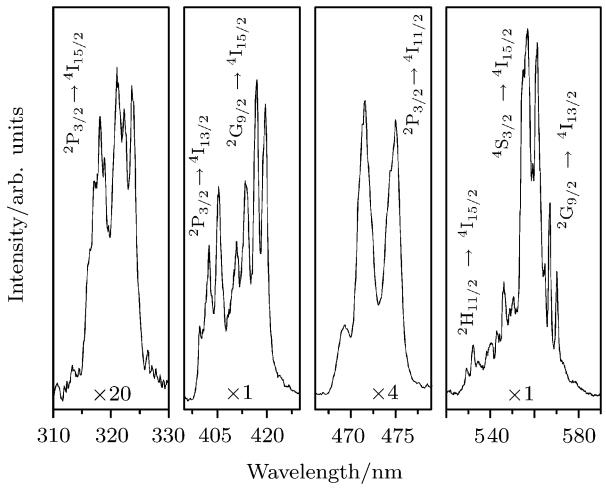


Fig.2. Upconversion luminescence spectrum under 647.2 nm excitation of $^4F_{9/2}$. The numbers below the spectra are the intensity amplification multiples of the corresponding spectra.

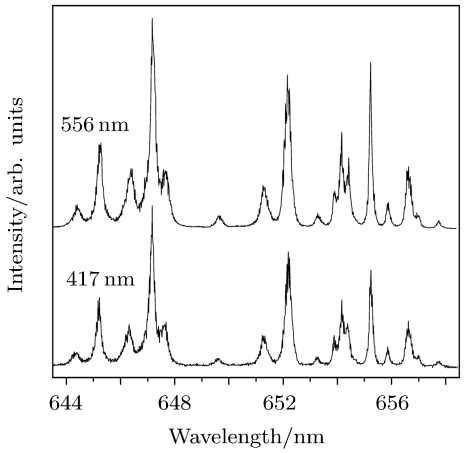


Fig.3. Excitation spectra for 417 nm and 556 nm upconversion luminescence.

Figures 4(a) and 4(b) shows the luminescence decay curves at 417, 535, 556 and 567 nm. By comparison between decay profiles at 417 and 567 nm, it is seen that they are the same and both of them come from $^2G_{9/2}$ decay. The emissions around 535 and 556 nm are from the thermalized energy levels $^2H_{11/2}$ and $^4S_{3/2}$ respectively and they have the same decay behaviour at room temperature.[19] The luminescence decay curves at 321, 405 and 472 nm from $^2P_{3/2}$ are shown in Fig.4(c). In Ref.[17] the decay profile at 410 nm has been recorded and attributed to the two transitions $^2P_{3/2} \rightarrow {}^4I_{13/2}$ and $^2G_{9/2} \rightarrow {}^4I_{15/2}$. But in this paper we found the difference of decay profiles between 405 and 417 nm, which indicates that violet emission around 405 nm comes from $^2P_{3/2}$ while that around 417 nm from $^2G_{9/2}$. Moreover, we observed that the green emission around 567 nm from $^2G_{9/2}$ not found in Ref.[17].

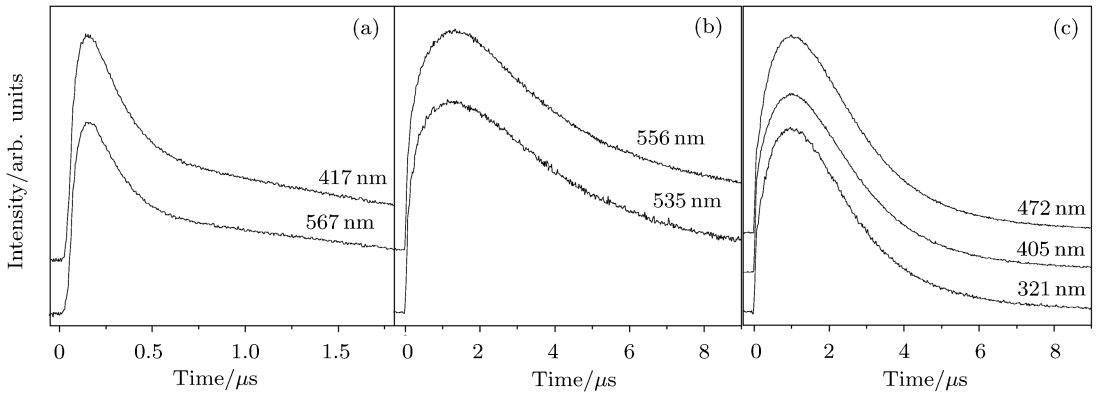


Fig.4. Decay curves of upconversion luminescence: (a) 417 and 567 nm, (b) 535 and 556 nm and (c) 321, 405 and 472 nm.

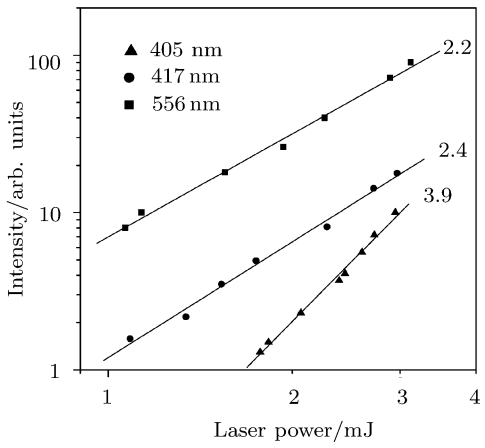


Fig.5. Dependence of upconversion luminescence intensity on pump power. The numbers denote the slopes in double-logarithmic representation.

The well-known upconversion mechanisms are excitation state absorption (ESA) and energy transfer upconversion (ETU), which can be distinguished by analyses of the time-resolved decay curves.[20,21] ESA process will be accomplished during the excitation pulse, while ETU can persist after the excitation pulse for a longer period which is related to the lifetime of the level providing energy transfer. Therefore, the ESA upconversion luminescence relaxation will exhibit a decay behaviour just like that induced by direct resonant excitation, while the ETU luminescence curve generally consists of a rise time section followed by decay section. It can be clearly seen that a clear rise time appears on every curve in Fig.4. This demonstrates that the upconversion luminescence at these positions are caused by ETU processes while ESA processes can be ruled out. Possible ETU transitions for the observed upconversion luminescence are proposed in Fig.1. For validation, dependence of upconversion luminescence intensity on pumping laser intensity was

measured and shown in Fig.5. From the slopes it can be supported that the $^2G_{9/2}$ and $^4S_{3/2}$ luminescence are induced by one-step ETU process while the $^2P_{3/2}$ luminescence by two-step ETU process as shown in Fig.1.

For the $^4S_{3/2}$ level, we agree that three possible paths $^4I_{11/2}+{}^4I_{11/2} \rightarrow {}^4F_{7/2} + {}^4I_{15/2}$, $^4I_{11/2}+{}^4I_{9/2} \rightarrow {}^4I_{15/2} + {}^4F_{5/2}$ and $^4I_{11/2} + {}^4I_{9/2} \rightarrow {}^4F_{5/2} + {}^4I_{15/2}$ referred by Ref.[17] result in the population of the $^4S_{3/2}$ level emitting green fluorescence. Its decay curve at 556 nm can be theoretically fitted by the expression for one-step ETU process[22]

$$N(t) = A[\exp(-t/\tau_{\rm d}) - \exp(-t/\tau_{\rm r})], \qquad (1)$$

where A is a constant, $\tau_{\rm d}$ and $\tau_{\rm r}$ are the decay and rise times respectively. Figure 6(a) shows the theoretically fitted curve of Eq.(1) to the results of measurement. It can be seen that the fitted curve is in good agreement with the results of measurement. In fitting calculations, $\tau_{\rm r}$= 0.73 μs and $\tau_{\rm d}$ = 5.9 μs were obtained. Obviously, the decay time is much longer than the lifetime (1.6 μs) of the $^4S_{3/2}$ level measured under direct excitation, which indicates that ETU is responsible for the population of the $^4S_{3/2}$ level.

In Ref.[17], the authors pointed out that the decay curve at 410 nm with a fast decay and a slow decay was attributed to the contribution of both $^2G_{9/2}$ and $^2P_{3/2}$ emission. In this paper, by using a monochromator of higher resolution, the decay curves at 417 and 405 nm were recorded as shown in Figs.4(b) and 4(c), which are obviously different. This fact was not observed or indicated in Ref.[17]. According to the Stark level data,[18] 417 nm radiation can only be attributed to the emission from $^2G_{9/2}$. The 417nm decay curve consists of a faster decay and a slower decay besides a risen part, which is very similar to that at 410 nm referred by Ref.[17]. The faster decay at 417 nm indicates that the population of $^2G_{9/2}$ originates from the possible ETU processes $^4I_{9/2} + {}^4I_{9/2} \rightarrow {}^2G_{9/2} + {}^4I_{15/2}$, $^4F_{9/2} + {}^4I_{9/2} \rightarrow {}^2K_{15/2} + {}^4I_{15/2}$ and $^4I_{9/2}+{}^4F_{9/2} \rightarrow {}^2K_{15/2}+{}^4I_{15/2}$ referred by Ref.[17]. But the slower decay indicates that the population of $^2G_{9/2}$ is induced by other ETU process not referred in Ref.[17], which originates from the levels with longer lifetime than $^4F_{9/2}$ and $^4I_{9/2}$. According to the energy level data,[18] it is found that the energy gap (17553 − 17911 cm^{-1}) of $^2G_{7/2}-{}^4I_{11/2}$ can be resonant with that (17820 − 18459 cm^{-1}) of $^4S_{3/2}-{}^4I_{15/2}$. Therefore, the ETU $^4I_{11/2} + {}^4S_{3/2} \rightarrow {}^2G_{7/2} + {}^4I_{15/2}$ is possible for the population of $^2G_{9/2}$. The longer lifetime of $^4I_{11/2}$ induces a slower decay by this ETU process.

The risen part and the faster decay part of 417 nm decay curve can also be theoretically fitted by Eq.(1). The theoretically fitted curve was shown in Fig.6(b), $\tau_{\rm r}$= 0.07 μs and $\tau_{\rm d}$= 0.56 μs were obtained. By exponential fitting for the slower decay part, $\tau_{\rm d}$= 2.21 μs was obtained, which is longer than the lifetimes of $^4F_{9/2}$ and $^4I_{9/2}$ (1.2 μs and 53 ns respectively) indicating that the luminescence at the slower decay part originates from the ETU process through the $^4I_{11/2}$ level but not through the $^4F_{9/2}$ and $^4I_{9/2}$ levels.

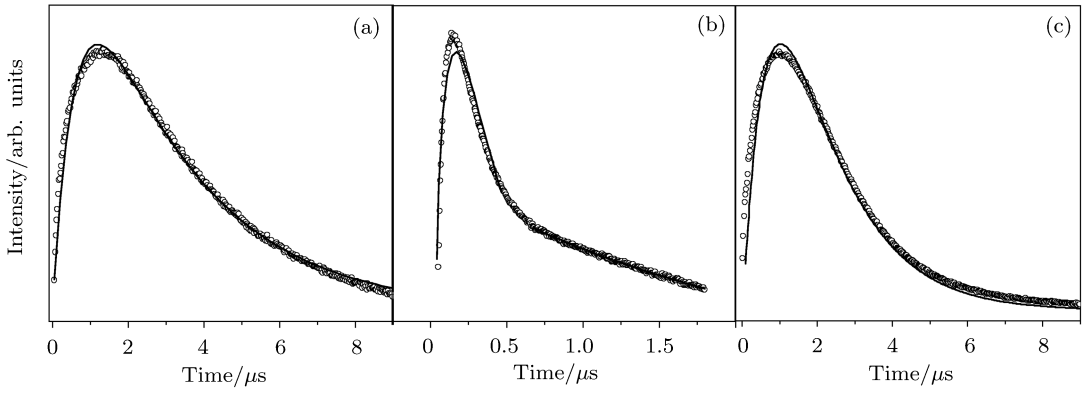


Fig.6. Experimental and theoretical decay curves: (a) 556 nm, (b) 417 nm and (c) 405 nm. The symbols correspond to experimental data and the solid lines represent the fitted results.

The second steps of ETU $^4S_{3/2}+{}^4S_{3/2} \rightarrow {}^2H_{9/2}+{}^4I_{15/2}$ and $^2H_{11/2}+{}^2H_{11/2} \rightarrow {}^4D_{5/2}+{}^4I_{15/2}$ can populate $^2H_{9/2}$ and $^4D_{5/2}$ respectively, then the quick nonradiative relaxation from $^2H_{9/2}$ and $^4D_{5/2}$ leads to the population of $^2P_{3/2}$ from which upconversion emissions around 321 nm, 405 nm, and 472 nm occur.

The time dependence of $^2P_{3/2}$ population can be described as

$$\frac{dN_P}{dt} = -\frac{N_P}{\tau_P} + \frac{1}{2}WN_S^2, \quad (2)$$

where N_P and N_S are the population densities of $^2P_{3/2}$ and $^4S_{3/2}$, τ_P is the lifetime of $^2P_{3/2}$ and W is the energy transfer rate from $^4S_{3/2}$. Time dependence of $^4S_{3/2}$ population is described by Eq.(1). So the solution of Eq.(2) has the form

$$N_P = C\Big[\frac{\exp(-2t/\tau_d)}{\tau_P^{-1}-2\tau_d^{-1}} + \frac{\exp(-2t/\tau_r)}{\tau_P^{-1}-2\tau_r^{-1}} - \frac{2\exp(-(\tau_r^{-1}+\tau_d^{-1})t)}{\tau_P^{-1}-\tau_r^{-1}+\tau_d^{-1}} - \Big(\frac{1}{\tau_P^{-1}-2\tau_d^{-1}} + \frac{1}{\tau_P^{-1}-2\tau_r^{-1}} - \frac{2}{\tau_P^{-1}-\tau_r^{-1}-\tau_d^{-1}}\Big)\exp(-2t/\tau_P)\Big], \quad (3)$$

where C is a constant, τ_d and τ_r are the decay and rise times of $^4S_{3/2}$ respectively. Fig.6(c) shows the theoretical curve of Eq.(3) by fitting to the experimental curve at 405 nm. The fitting results gave a theoretical lifetime τ_P= 1.09 μs of $^2P_{3/2}$ which is in agreement with the measured lifetime 1.22 μs. The good agreements between theoretical and experimental decay profiles achieved by the kinetic analyses support that the one-step and two-step ETU processes proposed in this paper are responsible for the observed upconversion luminescence.

4. Conclusion

In conclusion, UV and visible upconversion luminescence have been observed in Er^{3+}:YAG under 647.2 nm $^4F_{9/2}$ excitation and the corresponding kinetics was analysed. Upconversion luminescence intensity dependence on pump power was recorded. The luminescence decay profiles measured for the $^4S_{3/2}$, $^2G_{9/2}$ and $^2P_{3/2}$ levels were fitted by the rate equation theory and the results support that the upconversion mechanisms are ETU processes. Some one-step ETU processes lead to the population of $^2H_{11/2}$, $^4S_{3/2}$ and $^2G_{9/2}$, while some two-step ETU processes populate the $^2P_{3/2}$ level inducing 321 nm upconversion emission, the shortest wavelength produced in this study.

Acknowledgement

The authors would like to thank Professor Siyuan Zhang for providing Er^{3+}:YAG crystal.

References

[1] Scheps R 1996 *Prog. Quant. Electron.* **20** 271
[2] Chen X B, Li M X, Sawanobori, Zeng Z and Nie Y X 2000 *Acta Phys. Sin.* **49** 2482 (in Chinese)
[3] Georgescu S, Toma O, Florea C and Naud C 2003 *J. Lumin.* **101** 87
[4] Wen L, Li S G, Huang G S, Hu L L and Jiang Z H 2004 *Chin. Phys.* **13** 0258
[5] Yang H G, Dai Z W, and Sun Z W 2006 *Chin. Phys.* **15** 1273
[6] Semashko V V, Joubert M F, Descroix E, Nicolas S, Abdulsabirov R Yu, Naumov A K, Korableva S L and Cefala A C 2000 *SPIE* **4061** 306
[7] Smith A, Martin J P D, Sellars M J, Manson N B, Silversmith A J and Henderson B 2001 *Opt. Commun.* **188** 219
[8] Su F N and Deng Z D 2006 *Chin. Phys.* **15** 1096
[9] Whitley T J, Millar C A, Wyatt R, Brierley M C and Szebesta D 1991 *Electron. Lett.* **27** 1785
[10] Bogdanov V K, Booth D J and Gibbs W E K 2003 *J. Non-Cryst. Solids* **321** 20
[11] Biswas A, Maciel G S, Friend C S and Prasad P N 2003 *J. Non-Cryst. Solids* **316** 393
[12] Tsuda M, Soga K, Inoue H, Inoue S and Makishima A 1999 *J. Appl. Phys.* **85** 29
[13] Reddy B R and Nash-Stevenson S K 1994 *J. Appl. Phys.* **76** 3896
[14] Xu W, Dai S, Toth L M, Del Cui G D and Peterson J R 1995 *J. Phys. Chem.* **99** 4447
[15] Kostritskii S M, Maring D B, Tavlykaev R F and Ramaswamy R V 2000 *Appl. Phys. Lett.* **76** 2161
[16] Zhang X, Yuan J, Liu X, Jouart J P and Mary G 1997 *Chem. Phys. Lett.* **273** 416
[17] Xu H L and Kröll S 2005 *J. Lumin.* **111** 191
[18] Gruber J B, Quagliano J R, Reid M F, Richardson F S, Hils M E, Seltzer M D, Stevens S B, Morrison C A and Allik T H 1993 *Phys. Rev.* B **48** 15561
[19] Yang Z, Huang S, Lü S and Chen B 2004 *J. Non-Cryst. Solids* **343** 154
[20] Hehlen M P, Frei G and Güdel H U 1994 *Phys. Rev.* B **50** 16264
[21] Riedener T, Egger P, Hulliger J and Güdel H U 1997 *Phys. Rev.* B **56** 1800
[22] Gharavi A and Mcpherson G L 1992 *Chem. Phys. Lett.* **200** 279